Limnol. Oceanogr., 52(1), 2007, 46–59

Biogeochemistry of the Tana estuary and delta (northern Kenya)

Steven Bouillon[1] *and Frank Dehairs*
Department of Analytical and Environmental Chemistry, Vrije Universiteit Brussel, Pleinlaan 2, B-1050 Brussels, Belgium

Laure-Sophie Schiettecatte and Alberto Vieira Borges
Unité d'Océanographie Chimique, MARE, Université de Liège, B-4000 Sart-Tilman, Belgium

Abstract

The estuarine mixing zone of the Tana River (northern Kenya) and an extensive deltaic area just south of the estuary were sampled in April 2004 with the aim of identifying the distribution, sources, and processing of particulate and dissolved organic carbon (POC, DOC) and inorganic carbon (DIC). C4 inputs from the catchment contributed ~50% to the POC pool in the Tana River and estuary, and in the mangrove creek water column and intertidal sediments. The $\delta^{13}C$ values of DOC, however, were typically much more negative than that of POC, indicating a substantially higher contribution by C3 and/or mangrove-derived carbon in the DOC pool. The undersaturation of O_2, high pCO_2, and the nonconservative nature of DIC and $\delta^{13}C_{DIC}$ suggest a strongly heterotrophic water column, particularly in the freshwater part of the Tana and in the tidal creeks in the delta, where high additional inputs of organic matter were observed. However, some of these sites showed $\delta^{18}O_{DO}$ signatures lower than the atmospheric equilibrium (i.e., +24.2‰) indicative of significant O_2 production by photosynthesis. Therefore, the heterotrophic signature in the water column is likely the result of a strong interaction with the large intertidal areas, whereby respiratory activity in sediments and in the overlying water column during tidal inundation leave a marked signature on the water column. This is confirmed by the covariation between salinity-normalized total alkalinity and DIC, whose slope indicates an important role for anaerobic diagenetic processes. If our data are representative for other large river systems in the region, current estimates are likely to underestimate suspended matter and both inorganic and organic C fluxes to the Indian Ocean from tropical east Africa.

Estuaries represent a biogeochemically active zone, significantly transforming terrestrial riverine inputs to the coastal zone. Processing of organic matter along the estuarine mixing zone and in tidal creeks has the potential to dramatically alter the quantity, sources, and composition of organic carbon before its export to the coastal zone and leads to a strongly heterotrophic water column, resulting in a high CO_2 efflux toward the atmosphere. Given the importance of riverine transport of organic and inorganic carbon (C) in the global C budget, a thorough understanding of carbon cycling in estuaries and the underlying driving forces remain a major challenge, in particular for the tropics, where >60% of the global riverine organic and inorganic C transport is thought to occur (Ludwig et al. 1996*a*). Moreover, mangrove forests form a conspicuous habitat in many tropical estuaries and deltas, and their high productivity could have a major influence on the carbon budget of the coastal zone (Jennerjahn and Ittekkot 2002). However, the actual amount of mangrove-derived C inputs to the coastal zone remains an open question because local mineralization and subsequent efflux of CO_2 to the atmosphere appears to be a quantitatively important but poorly studied process—at least in the mangrove sites studied so far (~50 mmol C m^{-2} d^{-1}, data compiled by Borges et al. 2003). Cai et al. (1999) described a model for C cycling in temperate salt marsh–dominated estuaries, whereby mineralization in intertidal sediments and exchange of inorganic carbon through pore-water movement and/or diffusion during high tide explained the apparent heterotrophic characteristics of a tidal creek water column. A similar scenario is likely to occur in mangrove systems, and the interplay between these intertidal areas and tidal creeks in carbon exchange has been suggested previously (Ovalle et al. 1990; Bouillon et al. 2003; Borges et al. 2003).

Rivers and estuaries are typically heterotrophic systems, and their CO_2 emission rates are significant on a regional and global scale (Frankignoulle et al. 1998; Richey et al. 2002; Borges 2005). Intense mineralization of organic matter is considered responsible for sustaining this net CO_2 efflux, but given that river systems may transport organic material of various sources, age, and reactivity, and that in situ production may be significant in some systems, much remains to be resolved regarding the sources of carbon being mineralized and which factors control mineralization. Studies on the isotopic composition of dissolved and particulate organic carbon (DOC and POC)

[1] To whom correspondence should be addressed (steven.bouillon@vub.ac.be).

Acknowledgments

SB is funded by a postdoctoral mandate from the Fund for Scientific Research (FWO-Vlaanderen). Financial support was provided by the FWO-Vlaanderen (contracts G.0118.02 and 1.5.070.05) and by the FNRS (contracts 1.5.066.03), where AVB is a research associate. George Ndiritu (National Museums, Nairobi) and Michael Korntheuer helped in the field, and Renaldo Retief and the staff of the Tana Delta Camp provided logistical help during our stay in the delta. James Syvitski and Albert Kettner provided sediment discharge data. David P. Gillikin, Steve Hamilton (associate editor), and two anonymous referees provided constructive comments to the article in manuscript.

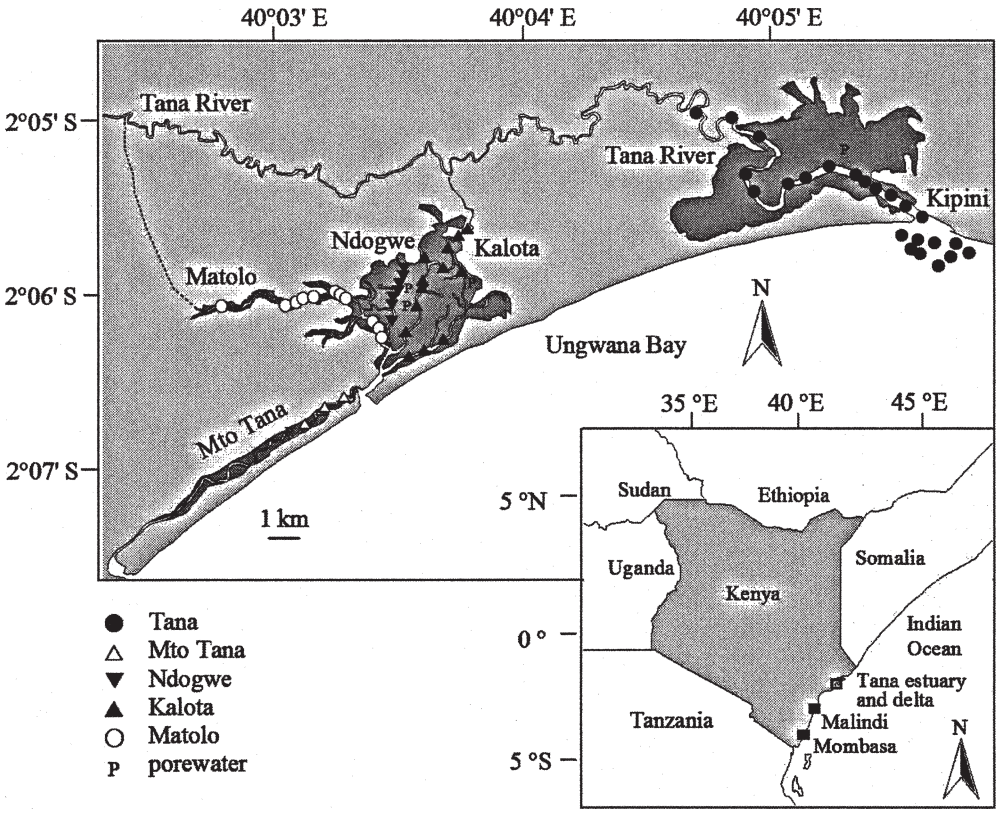

Fig. 1. Location of sampling area and detail of Tana estuary and delta. Sampling locations are indicated by various symbols, which correspond to those used in Figs. 3–6, 7C, 8, and 9. P represents locations where pore-water samples were taken in intertidal mangroves. Darkest areas show main mangrove-covered zones. Dotted line indicates existing connection between Matolo Creek and Tana River, for which the exact location is not known.

have revealed that ''old'' organic carbon can be rapidly mineralized once it enters aquatic systems (Cole and Caraco 2001), but on the other hand, there is clear evidence that DOC of younger age can be preferentially mineralized (Raymond and Bauer 2001). A recent study on the Amazon River system (Mayorga et al. 2005) suggested that the dominant source sustaining the net heterotrophy is in the form of a relatively small pool of contemporary organic matter, despite the significant contribution of much older carbon source in the total organic carbon pool.

The biogeochemistry of African river systems has to date received very little attention, with almost all available studies focusing on rivers draining western Africa (e.g., Niger, Senegal, Congo, and Sanaga Rivers; Martins and Probst 1992). The total lack of data on the sources, fluxes, and transformations of carbon in river systems along the tropical east African coastline (with several large river systems such as the Tana, Rufiji, and Zambezi, with average freshwater discharges of 156, 779, and 3,341 $m^3 s^{-1}$, respectively; data from the Global River Discharge database, available at http://www-eosdis.ornl.gov/RIVDIS/rivdis.html) therefore represents one of the major gaps in our knowledge on carbon dynamics in the tropical coastal zone. Here, we examined the sources and dynamics of organic and inorganic carbon and a range of physicochemical parameters in one of the three largest tropical east African river systems: the Tana River, situated in northern Kenya, as well as in a number of tidal creeks situated in a connected deltaic system located directly south of the main Tana estuary.

Materials and methods

Study sites—The Tana River originates in the vicinity of Mount Kenya and is the longest river system in Kenya (~1,000 km), with a catchment area of ~120,000 km^2. An average of 4×10^9 m^3 of freshwater is discharged annually, with peak flows occurring between April and June and a shorter high flow period during November–December. The sediment discharge carried by the Tana River has been estimated at 3.1 to 6.8 $\times$ 10^9 kg yr^{-1} (Syvitski et al. 2005 and Kitheka et al. 2005, respectively). The river enters the Indian Ocean roughly midway between Malindi and Lamu, near Kipini (Fig. 1), but part of the freshwater flow branches off into a complex network of tidal creeks, savanna-like floodplains, coastal lakes, and mangrove swamps known as the Tana Delta. The delta has no permanent human settlements and covers ~1,300 km^2, with a ridge of high sand dunes shielding it from Ungwana Bay. The current Tana River mouth in Kipini used to be the mouth of a much smaller estuary (known as Osi or Ozi), but was connected to the Tana River after a man-made

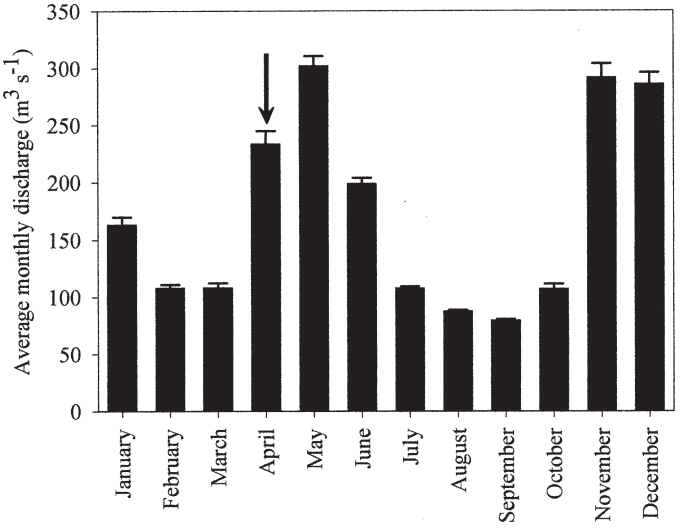

Fig. 2. Average monthly discharge data for Tana River, measured at Garissa during 1982–1996 (i.e., after construction of several dams along rivercourse). Data from Maingi and Marsh (2002). Error bars represent 1 SE.

canal broke through at the end of the 19th century, thereby connecting the Tana and Ozi Rivers (Denhardt and Denhardt 1884). The former Tana River mouth ("Mto Tana"; Fig. 1) thereby lost most of its water supply (Sampson 1933) and has now become a narrow creek only navigable at spring high tide. During the 1960s, a new breakthrough occurred in the sand dunes near Shekiko (R. Retief pers. comm.), further increasing the seawater influence in the delta. Furthermore, the construction of several dams along the rivercourse during the 1980s resulted in a reduced average freshwater supply (Maingi and Marsh 2002). Kalota Creek (Fig. 1) formerly received freshwater from the Tana River, but this connection was artificially disrupted in 1982 to counter the brackish water intrusion in nearby rice paddies. The only freshwater inputs we could establish at the time of sampling occurred via Matolo Creek (*see* Fig. 1), although the actual location of its connection to the Tana appears to be unknown even locally.

Our sampling took place during a 3-week period in April 2004, and even though no discharge data could be obtained for recent years, this period typically shows intermediate discharge rates and represents the onset of a high-flow period (Fig. 2). Extensive floodplains consisting of tall mangrove forests (mainly *Avicennia marina* and *Heritiera littoralis*, with some *Rhizophora mucronata*) border the Tana estuary mouth, but the estuary has no major side creeks. The southern delta, however, comprises a network of tidal creeks intersecting a mixed landscape of mangrove forests (dominated by *Avicennia marina* and *Ceriops tagal*), salt pans, and savanna grasslands. The Kenyan coast experiences semidiurnal tides, with a maximum tidal range of ~4 m (Colombini et al. 1995). Surface water was sampled at 65 stations situated along the Tana River (from the freshwater part to the river plume), and in the various creeks of the Tana Delta. In addition, pore water was sampled at seven locations in the intertidal mangrove areas (Fig. 1).

Sampling and analytical techniques—Fieldwork took place during a 3-week period in April 2004. Surface water for field measurements of dissolved O_2, pH, temperature, and salinity were taken with a Niskin bottle from ~0.5 m below the surface. Oxygen saturation level ($\%O_2$) was measured immediately after collection with a polarographic electrode (WTW Oxi-340) calibrated on saturated air, with an accuracy of ±1%. pH was measured by a Ross-type combination electrode (ORION) calibrated on the NBS (U.S. National Bureau of Standards) scale, as described by Frankignoulle and Borges (2001), with a reproducibility of ±0.005 pH units. Samples for determination of total alkalinity (TA) were obtained by prefiltering 100 mL of water through precombusted Whatman GF/F filters, followed by filtration through 0.2-μm Acrodisc syringe filters, and were stored in HDPE bottles until analysis by automated electrotitration on 50 mL samples with 0.1 mol L^{-1} HCl as titrant (reproducibility estimated at ±2 μmol kg^{-1}). The partial pressure of CO_2 (pCO_2) and total dissolved inorganic carbon (DIC) concentrations were computed from pH and TA measurements with the thermodynamic constants described in Frankignoulle and Borges (2001), and the accuracy of computed DIC and pCO_2 values are estimated at ±5 μmol kg^{-1} and ±5 ppm, respectively. Water samples for the analysis of $\delta^{13}C_{DIC}$ and $\delta^{18}O_{DO}$ were taken from the same Niskin bottle by gently overfilling 10- or 20-mL glass headspace vials, respectively, poisoning with 20 μL of a saturated $HgCl_2$ solution, and gas-tight capping with a butyl rubber plug and aluminum cap. For the analysis of $\delta^{13}C_{DIC}$, a He headspace was created, and ~300 μL of H_3PO_4 was added to convert all inorganic carbon species to CO_2. After overnight equilibration, part of the headspace was injected into the He stream of an elemental analyzer–isotope ratio mass spectrometer (EA-IRMS, ThermoFinnigan Flash1112 and ThermoFinnigan Delta+XL) for $\delta^{13}C$ measurements. The obtained $\delta^{13}C$ data were corrected for the isotopic equilibration between gaseous and dissolved CO_2 by using the algorithm presented in Miyajima et al. (1995). For $\delta^{18}O_{DO}$, a similar headspace was created in the 20-mL vials, after which they were left to equilibrate for 2 h. $\delta^{18}O_{DO}$ was then measured with the same EA-IRMS setup by monitoring *m/z* 32, 33, and 34 and using a molecular sieve (5 Å) column to separate N_2 from O_2. Outside air was used as the internal standard to correct all $\delta^{18}O$ data.

Samples for Ca^{2+} and Mg^{2+} were obtained by prefiltering surface water through precombusted glass fiber filters (Whatman GF/F, 0.7 μm), further filtration through 0.2-μm Acrodisc syringe filters, and preservation with 10 μL of ultrapure HNO_3. Concentrations of Ca^{2+} and Mg^{2+} were measured by inductively coupled plasma–atomic emission spectrometry with a reproducibility better than 3%. Samples for PO_4^{3-} were similarly obtained and preserved with $HgCl_2$ (1 μL mL^{-1} sample). Samples for Si were prepared by prefiltration through 0.45-μm Sartorius filters, further filtration through 0.2-μm Acrodisc syringe filters, and preservation with 100 μL of HCl (30%) for 20 mL of sample. PO_4^{3-} and Si were analyzed by standard colorimetric methods (Grasshoff et al. 1983), with a precision of ±0.1 μmol L^{-1}.

Samples for total suspended matter (TSM) were stored in a cool box before collection on preweighed and precombusted (overnight at 450°C) 47 mm Whatman GF/F filters, which were subsequently dried. For nonfreshwater stations, filters were briefly rinsed with mineral water to remove the contribution by salts. Samples for particulate organic carbon (POC), particulate nitrogen (PN), and $\delta^{13}C_{POC}$ were filtered on precombusted 25 mm Whatman GF/F filters and dried. These filters were later decarbonated with HCl fumes under partial vacuum for 4 h, redried, and packed in Ag cups. POC and PN were determined on the above-mentioned EA-IRMS with acetanilide used as a standard. Reproducibility of $\delta^{13}C_{POC}$ measurements was better than 0.2‰. Samples for dissolved organic carbon (DOC) and $\delta^{13}C_{DOC}$ were obtained as described above for nutrients, and were preserved by the addition of 50 μL of H_3PO_4 per 15 mL of sample. DOC and $\delta^{13}C_{DOC}$ were measured with a custom-modified Thermo HiPerTOC total organic carbon analyzer, interfaced to the IRMS via the Conflo III interface (Bouillon et al. 2006). Briefly, DOC in up to 15 mL of sample was converted to CO_2 with a combined UV–persulfate oxidation method in a heated reactor, and the resulting CO_2 was bubbled out by a helium stream, purified in a custom reduction/oxidation column at 680°C, passed over a GC column and transferred to the IRMS for quantification and stable isotope measurements. Typical reproducibility was in the order of ±5% for DOC, and ±0.25‰ for $\delta^{13}C_{DOC}$. Samples for chlorophyll *a* (hereafter Chl *a*) were obtained by filtering a known volume of surface water on glass fiber filters (0.7 μm, Whatman GF/F) and were stored at −20°C. Pigments were extracted for approximately 12 h in 15 mL of 90% acetone at 4°C and analyzed with a Turner TD-700 Fluorometer, with an accuracy of ±4%.

Primary production measurements were carried out at selected stations by incubating surface water in borosilicate bottles tied to the boat just below the water surface for ~2 h. The incubation bottles were spiked with 500 μL of a 20 μmol L^{-1} $NaH^{13}CO_3$ solution. After incubation, the water was poisoned by adding 200 μL of a saturated $HgCl_2$ solution. Upon return in the field laboratory, duplicate samples were filtered on precombusted 25-mm Whatman GF/F filters for the determination of POC and $\delta^{13}C_{POC}$, and duplicate water samples were taken as described above for the determination of $\delta^{13}C_{DIC}$. Average values of $\delta^{13}C_{DIC}$, POC, and $\delta^{13}C_{POC}$ were used to calculate the uptake rate of C. Pelagic community respiration rates (R) were estimated at selected stations by incubating three replicate borosilicate bottles filled from the Niskin bottle in a darkened cool box filled with surface water to retain the ambient temperature as well as possible. DO concentrations were measured after ~24 h and compared with the field measurements of $\%O_2$ at the relevant station to calculate R.

At selected stations inside the intertidal mangrove forest, pore water was sampled by extracting a sediment core (~50 cm deep) and immediately pumping up the inflowing water under partial vacuum. $\%O_2$, pH, and temperature were measured directly after collection in the field; porewater samples for other dissolved parameters were stored in a cool box and processed upon return in the field laboratory.

Results

Much of the salinity gradient of the Tana was found in the river plume beyond the mouth of the estuary. In the southern delta, freshwater conditions were encountered upstream along Matolo Creek; the other creeks had salinities between 13 and 34. With few exceptions, the water column was strongly undersaturated in O_2 (Fig. 3A). $\%O_2$ in the Tana was lowest in the freshwater end (~60–70%) and increased gradually toward the plume, where values reached near-saturation levels. A similar increase was observed along the salinity gradient of Matolo Creek, but with $\%O_2$ values consistently lower than along the Tana (Fig. 3A). Mangrove pore waters were consistently found to be anoxic, with $\%O_2$ measured immediately after collection (which may have introduced some oxygen; *see* Materials and Methods) typically <5% (data not shown on the figures). pH in the freshwater end of the Tana ranged between 7.41 and 7.51 (Fig. 3B), and increased gradually toward the plume (up to 8.58). A similar increase was noted along Matolo Creek, but with consistently lower pH when compared with the Tana transect (Fig. 3B). pH values in the tidal creeks were markedly lower than at similar salinity levels along the Tana or Matolo. Mangrove pore waters consistently showed very low but variable pH (6.51–7.06), regardless of pore-water salinity (Fig. 3B).

TA along the Tana salinity gradient ranged between 1.667 and 2.163 mmol kg^{-1} in the freshwater reaches and generally increased toward the plume (2.009–2.163 mmol kg^{-1}, Fig. 3C). However, several stations in the freshwater and oligo- and mesohaline region showed apparent internal production of TA (up to ~0.3 mmol kg^{-1}). Although TA in the freshwater part of Matolo (1.589 mmol kg^{-1}) was even lower than in the freshwater part of the Tana, TA along the salinity gradient in Matolo was consistently higher than along the Tana transect by ~0.2 mmol kg^{-1} and showed an overall nonconservative behavior (i.e., internal production of TA). In the tidal creeks of the delta, TA similarly behaves in a nonconservative way, with either a depletion in TA (in some of the stations at Ndogwe and Kalota creeks) or excess TA (Ndogwe, Kalota, and Mto Tana). All pore waters from the Tana and delta showed very high TA (2.738–12.893 mmol kg^{-1} along the Tana, 3.373–4.445 mmol kg^{-1} in the delta, Fig. 3C). The pattern observed in DIC generally follows that of TA (data not shown). CO_2 showed a strong oversaturation in the freshwater part of the Tana River (4,000–5,300 ppm), decreasing rapidly toward the river plume, where it reached values near equilibrium (Fig. 3D). Compared with the Tana, pCO_2 values in Matolo Creek and the mangrove creeks of the delta were much higher at comparable salinity levels, with an overall average of 2,600 ± 1,750 ppm. $\delta^{13}C_{DIC}$ shows a typical freshwater-marine trend along the Tana and Matolo (Fig. 3E). The $\delta^{13}C_{DIC}$ data from the tidal creeks in the delta confirm the nonconservative behavior of DIC, with typically more negative values than expected from under a conservative mixing scenario (Fig. 3E). Both Ca^{2+} and Mg^{2+} showed conservative

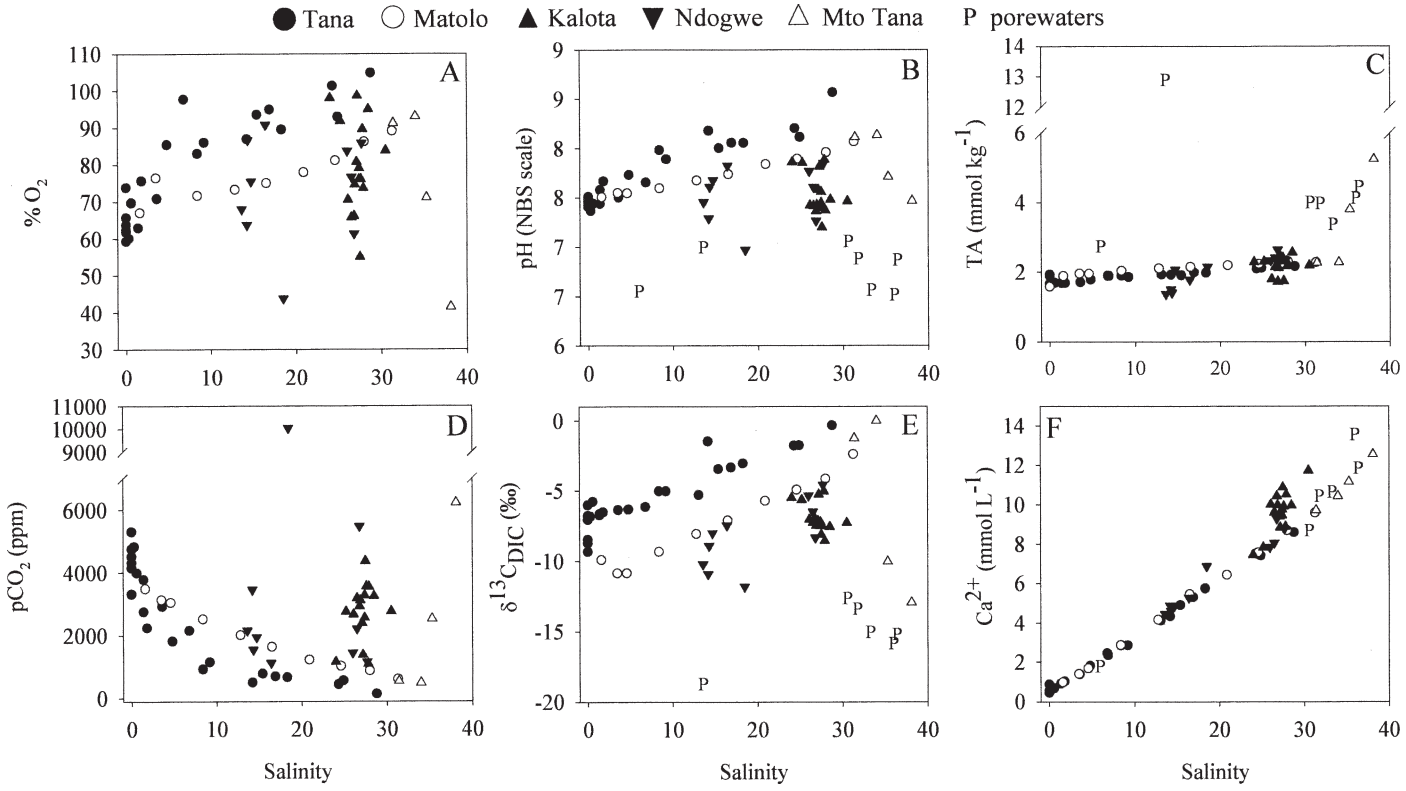

Fig. 3. Distribution of (A) oxygen saturation level, (B) pH, (C) total alkalinity, (D) pCO_2, (E) $\delta^{13}C_{DIC}$, and (F) Ca^{2+} concentrations along salinity gradient of Tana estuary and Matolo Creek, and in tidal creeks of Tana Delta.

behavior along the salinity gradient of the Tana River and Matolo Creek (Fig. 3F). Several creeks and pore-water stations in the southern delta, however, showed a marked excess of Ca^{2+} (Mg^{2+}, in contrast, was conservative throughout), reaching +1.41 ± 0.79 mmol L^{-1} for Kalota Creek and +0.92 ± 1.19 mmol L^{-1} for the mangrove pore-water samples.

$\delta^{18}O_{DO}$ values ranged overall between +21.2 and +33.6‰, and correlated inversely with $\%O_2$ (Fig. 4), consistent with isotope discrimination during O_2 consumption (i.e., leading to an ^{18}O-enriched residual O_2 pool) and inputs of isotopically light O_2 produced by photosynthesis.

TSM concentrations (Fig. 5A) showed a rather erratic pattern along the salinity gradient of the Tana and Matolo Creek, with highest but highly variable levels in the freshwater part of the Tana (802 ± 464 mg L^{-1}) and at salinities between 5 and 10. At salinities higher than 20, TSM concentrations were generally low (typically < 50 mg L^{-1}), except for Kalota Creek where TSM averaged 140 ± 145 mg L^{-1} and with maxima up to 660 mg L^{-1}. The distribution of POC was generally similar to that of TSM, with highest values in the freshwater part of the Tana (8.61 ± 4.52 mg L^{-1}), a general decrease toward the plume but with some sporadic maxima, and with a local increase in POC levels in some of the tidal creeks, particularly in Kalota where POC averaged 2.64 ± 2.34 mg L^{-1} (Fig. 5B). The contribution of POC to the total TSM pool was typically low (generally between 1% and 2%), but somewhat higher in some of the tidal creeks (up to 4.5%). POC : PN (atom) ratios averaged 7.5 ± 1.0 ($n = 65$) and showed no distinct pattern along the salinity gradient or between the different subareas sampled (Fig. 5C). $\delta^{13}C_{POC}$ (Fig. 5D) in the freshwater part of the Tana ranged from −22.3 to −21.0‰ and changed little over the entire salinity gradient, except for a marked

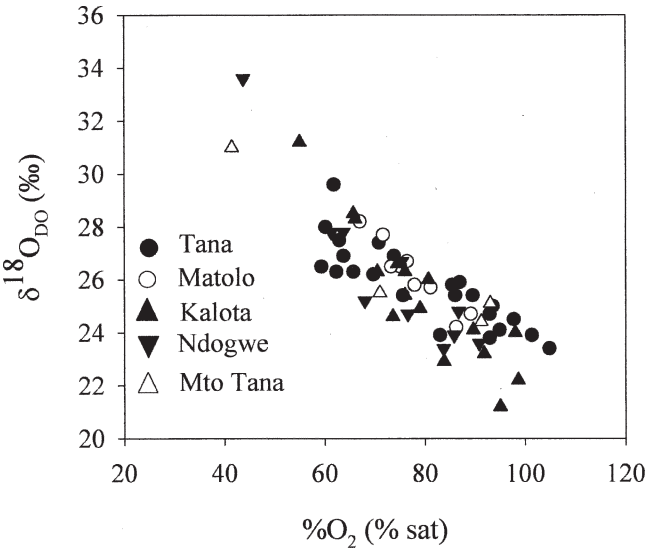

Fig. 4. Relationship between oxygen stable isotope composition of dissolved oxygen ($\delta^{18}O_{DO}$) and oxygen saturation levels for all surface-water samples.

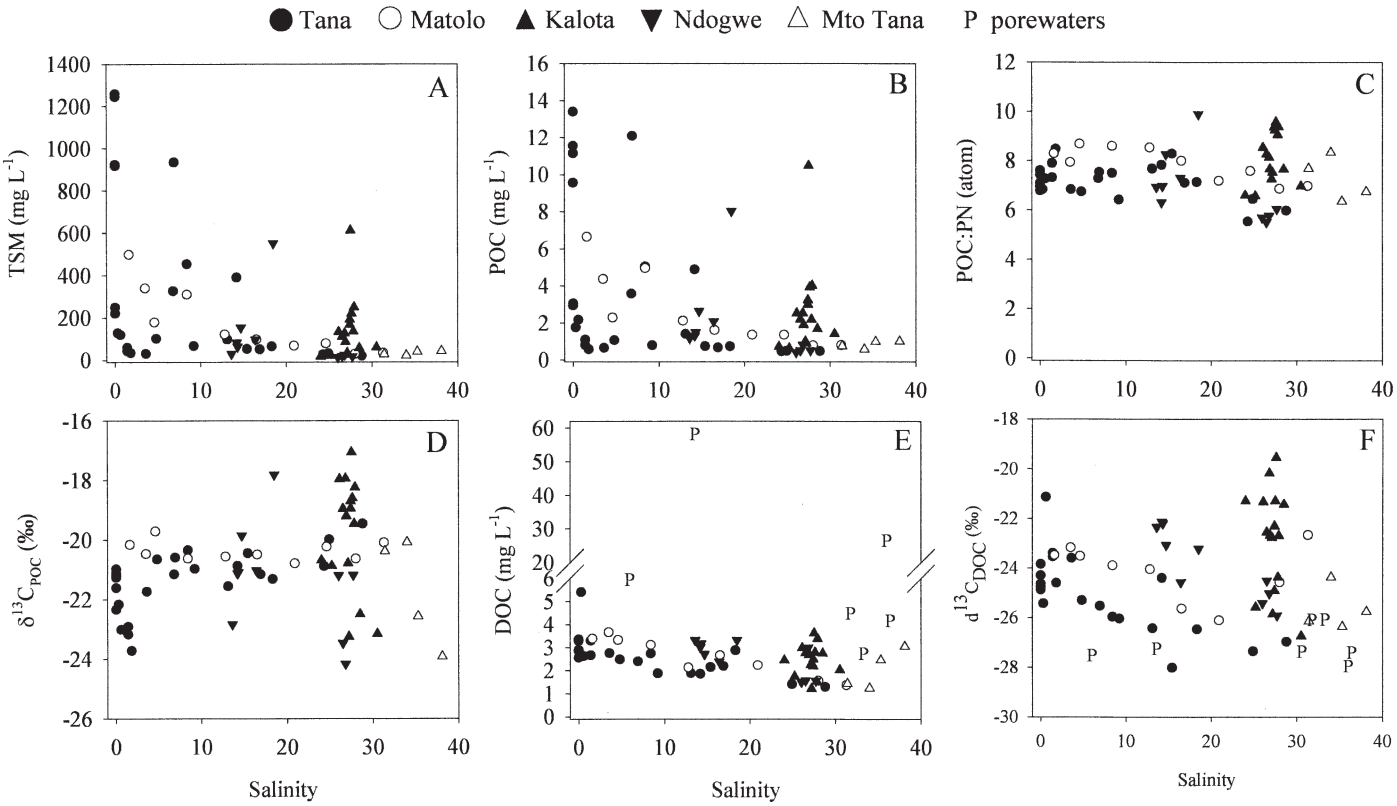

Fig. 5. Distribution of (A) total suspended matter, (B) POC, (C) POC : PN ratios (atom : atom), (D) $\delta^{13}C_{POC}$, (E) DOC, and (F) $\delta^{13}C_{DOC}$ along salinity gradient of Tana estuary and Matolo Creek, and in tidal creeks of Tana Delta.

decrease to approximately −24 to −23‰ in the salinity range between 0.5 and 2. In contrast to our expectation that mangrove inputs in the delta would consistently lower $\delta^{13}C_{POC}$ signatures, the tidal creeks showed on average similar $\delta^{13}C_{POC}$ values, albeit with a much wider range (−24.2 to −17.1‰).

DOC concentrations (Fig. 5E) in the water column ranged between 1.3 and 5.4 mg L^{-1} for the Tana estuary, between 1.4 and 3.7 mg L^{-1} for Matolo Creek, between 1.2 and 3.6 mg L^{-1} for the rest of the delta, and were typically much higher for mangrove pore waters (2.7–58.1 mg L^{-1}). Salinity profiles of DOC do not show a distinct pattern along the Tana or Matolo, but do demonstrate high inputs of DOC in the tidal creeks of the delta (Fig. 5E). However, DOC : POC ratios (which ranged between 0.2 and 4.2) showed a clear logarithmic relationship with TSM concentrations (Fig. 6), as has been proposed for rivers worldwide in previous studies (Ittekkot and Laane 1991), and this indicates that turbidity exhibited a major control on the relative DOC and POC distribution. The $\delta^{13}C$ profile of DOC was distinctly different from the $\delta^{13}C_{POC}$ pattern: $\delta^{13}C_{DOC}$ values were in most cases significantly more negative than $\delta^{13}C_{POC}$, and for the Tana estuary, $\delta^{13}C_{POC}$ showed a slight increase with salinity, whereas $\delta^{13}C_{DOC}$ showed a distinct decrease with increasing salinity (Fig. 5F, 7).

Chl *a* concentrations (Fig. 8A) along the Tana ranged typically between 0.7 and 3 μg L^{-1}, with a few erratic maxima. Concentrations in Matolo were similar, but with a consistent increase toward the euhaline zone. Chl *a* concentrations in the tidal creeks of the delta (Kalota, Ndogwe, and Mto Tana) were consistently higher, ranging typically between 2 and 8 μg L^{-1} (Fig. 8A). Consequently,

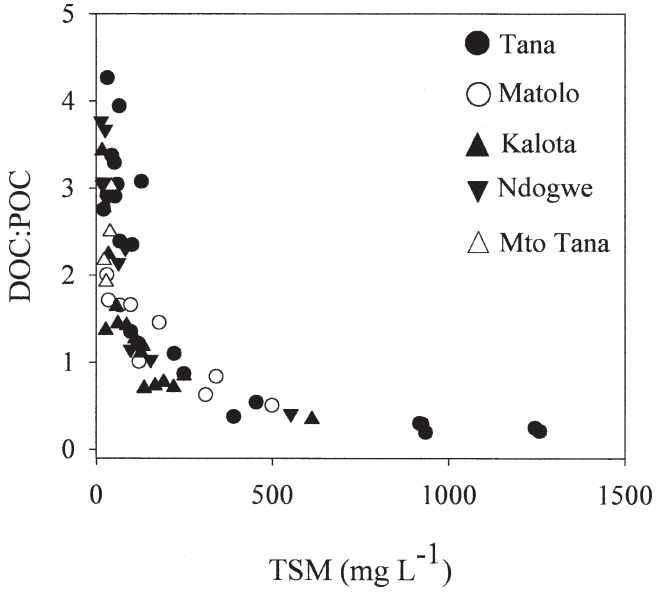

Fig. 6. Relationship between total suspended matter load (TSM) and ratio of dissolved to particulate organic carbon (DOC : POC) for various sampling regions.

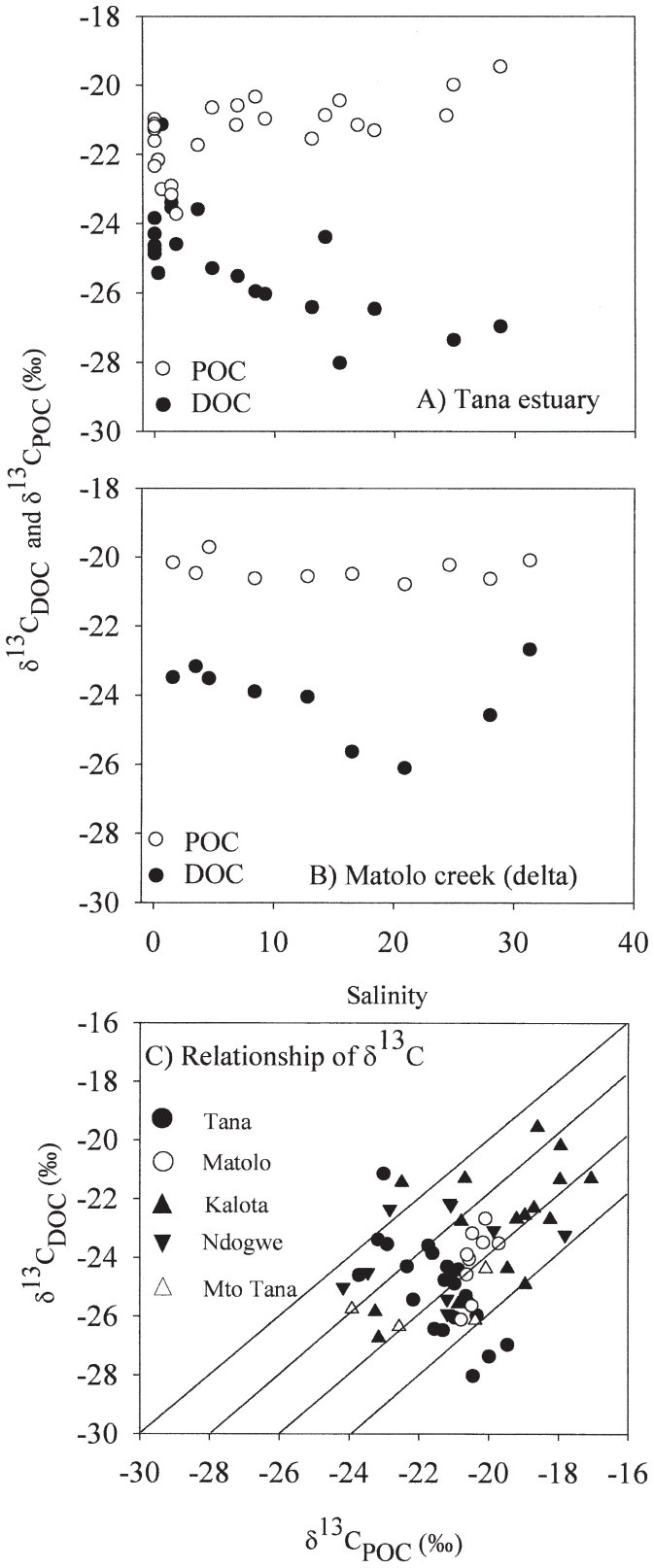

Fig. 7. Comparison of $\delta^{13}C$ signatures of POC and DOC along salinity gradient of Tana (A) and Matolo (B), and relationship between $\delta^{13}C$ signatures of POC and DOC for different sampling areas (C).

POC : Chl *a* ratios (Fig. 8B) were high in the Tana and Matolo (with highest values between 1,200 and 6,800 in the freshwater part), and lower in the delta creeks (430 ± 380).

Silica in the Tana increased significantly from freshwater to a salinity of 2, and roughly followed conservative mixing behavior in the mesohaline region (Fig. 9A). Silica concentrations in Matolo were similar to those in the Tana at equivalent salinities but were higher in Kalota, Mto Tana and pore waters than those in the Tana at equivalent salinities. Silica concentrations in Ndogwe are either higher or lower than in the Tana at equivalent salinities. Trends in phosphate as a function of salinity are generally similar to those of silica although they show more scatter (Fig. 9B).

A limited number of subsurface pelagic community respiration and primary production measurements were made at selected stations (Table 1). Respiration rates ranged between 7.8 and 23.9 μmol O_2 L^{-1} d^{-1}, but the small number of samples did not allow us to discern any patterns in these data. Instantaneous primary production measurements taken along the Tana River varied between 0.12 and 2.03 μmol C L^{-1} h^{-1} (average 0.77 ± 0.63 μmol C L^{-1} h^{-1}, $n = 7$) and showed no correlation with any of the other variables. In the delta, primary production showed a wider range and was on average higher than along the Tana (1.28 ± 0.85 μmol C L^{-1} h^{-1}, $n = 10$).

Discussion

Transport of organic and inorganic carbon to the Indian Ocean—Data on the carbon export fluxes from African rivers are particularly scarce. For the tropics, data are only available from systems draining the west coast, hence global extrapolations include a large uncertainty (*see*, e.g., Schlünz and Schneider 2000). For the Tana River, the total annual sediment flux has recently been estimated at 6.8×10^9 kg yr^{-1} (Kitheka et al. 2005), but this estimate is more than twice as high as that used in the global compilation of data presented in Syvitski et al. (2005), i.e., 3.0×10^9 kg yr^{-1}. However, the discharge data set used in the calculations of Kitheka et al. (2005) covers ~1.5 yr of data and shows several peaks that may not be representative over longer terms, e.g., their average discharge rate of 230 m^3 s^{-1} is significantly higher than the reported average of 155 m^3 s^{-1} reported for the Tana at Garissa (University of New Hampshire, Global Runoff Data Centre database for a period of 42 yr). A rough calculation using our average TSM concentrations for all freshwater stations (802 mg L^{-1}) and multiplying this with the total average annual discharge (4×10^9 m^3) gives an estimate of annual suspended matter transport (3.21×10^9 kg yr^{-1}) remarkably close to that in the Syvitski et al. (2005) data set. Our sampling period (Fig. 2) typically falls within intermediate flow conditions and marks the onset of a higher discharge period. Despite the fact that we have not sampled over a seasonal basis, which might cause bias in the extrapolation of our data to annual estimates, the similarity in TSM flux estimates suggests that it would be reasonable to use the POC : TSM, DOC, and DIC data from the freshwater stations to derive a first approximation of carbon export rates from the Tana. These estimates (3.44

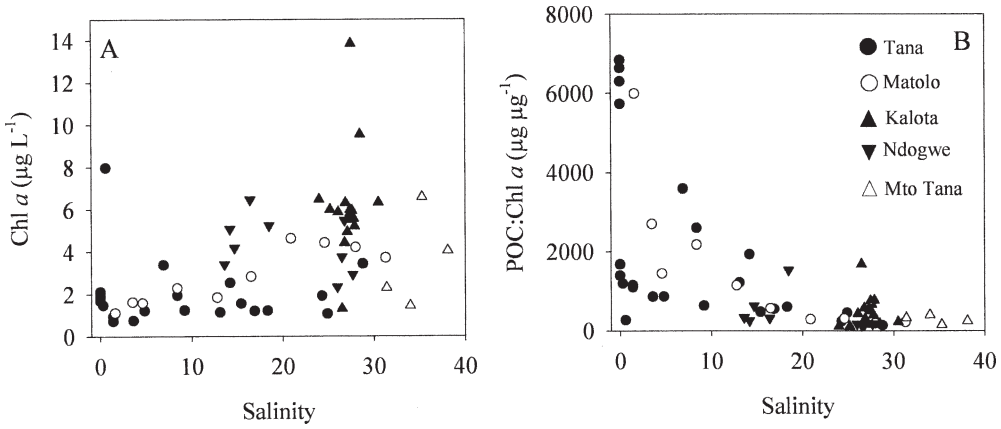

Fig. 8. Distribution of sestonic Chl and POC : Chl ratios along salinity gradient of Tana estuary and Matolo Creek, and in tidal creeks of Tana Delta.

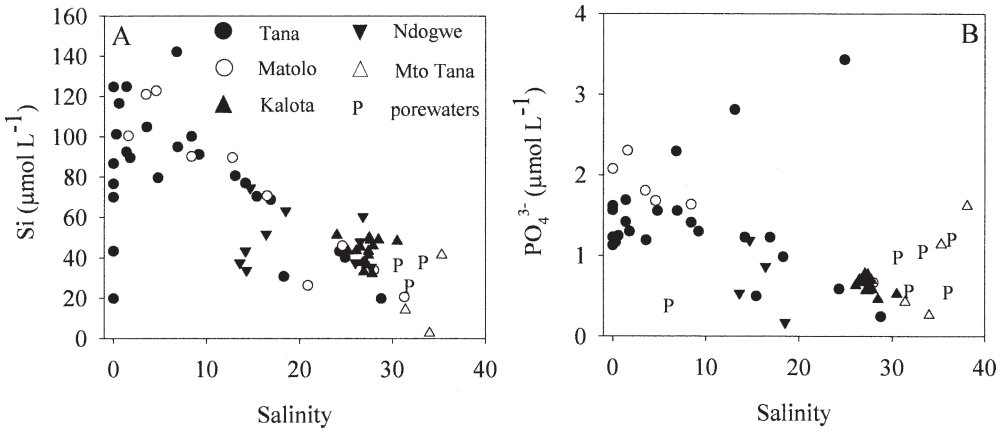

Fig. 9. Distribution of Si and PO_4^{3-} concentrations along salinity gradient of Tana estuary and Matolo Creek, and in tidal creeks of Tana Delta.

Table 1. Overview of instantaneous primary production (by ^{13}C incorporation) and respiration measurements (by O_2 evolution, in triplicate) in various parts of the Tana estuary and delta. Note that the reported rates are not depth integrated. n.d. = no data.

Location	Salinity	P (μmol C L^{-1} h^{-1})	R (μmol O_2 L^{-1} h^{-1})
Tana	0	0.60±0.30	0.95±0.13
Tana	0.3	2.03	n.d.
Tana	3.3	0.41	0.68±0.09
Tana	12.6	0.55	n.d.
Tana	15.0	0.12	n.d.
Tana	18.8	0.97	0.60±0.14
Kalota	25.5	1.27	0.33±0.02
Kalota	25.1	3.36	n.d.
Kalota	31.3	1.63	n.d.
Kalota	26.1	1.17	n.d.
Ndogwe	13.3	0.37	1.00±0.01
Ndogwe	14.0	1.69	n.d.
Ndogwe	24.8	1.07	0.61±0.04
Mto Tana	32.5	0.44	0.36±0.05
Matolo	29.7	0.77	n.d.
Matolo	20.2	1.05	0.35±0.04

$\times$ 10^{10} g POC yr^{-1}, 1.19 $\times$ 10^{10} g DOC yr^{-1}, and 9.4 $\times$ 10^{10} g DIC yr^{-1}) are roughly twice as high as those currently in use for the African continent when expressed per unit of discharge (Ludwig et al. 1996*a,b*; Schlünz and Schneider 2000). Moreover, it can be noted that the DIC : POC export ratio given here deviates substantially from that proposed by Ludwig et al. (1996*b*), where HCO_3^- export to the Indian Ocean between 0 and 4°S was estimated at ~20% of POC export, whereas our data indicate an almost three-fold *higher* export of inorganic carbon compared with POC.

The DOC : POC ratios found here in the freshwater and oligohaline part of the Tana are variable (1.4 ± 1.3) but are close to the ratio estimated by the Ludwig et al. (1996*b*) model for the region considered. Although the discrepancy between our estimates of DIC and organic carbon export (and their ratios) and those predicted by such models does not necessarily imply that the underlying principles of these models are incorrect (i.e., the discrepancy may arise from inadequate input data sets for this region), it is clear that a more thorough assessment of C transport in the Tana and other east African river systems is needed to better

Table 2. Overview of intertidal mangrove sediment characteristics (data from Bouillon and Boschker 2006): total organic carbon (%), elemental ratio (atom), $\delta^{13}C$ of sediment organic carbon, and $\delta^{13}C$ signature of bacterial phospholipid fatty acids i+a15 : 0. Note that there is a fractionation of approximately −3‰ to −6‰ between the bacterial C source and the i+a15 : 0 fatty acids (*see* Bouillon and Boschker 2006 for a discussion).

Location	%TOC	TOC : TN	$\delta^{13}C_{TOC}$	$\delta^{13}C_{i+a15:0}$
Tana	2.36±0.20	13.7±0.5	−25.6±0.3‰	−28.7±1.1‰
Ndogwe	1.06±0.07	11.9±0.5	−22.6±0.2‰	−26.7±1.3‰
Kalota (west)	1.11±0.07	10.2±0.2	−21.8±0.3‰	−26.4±0.6‰
Kalota (east)	1.09±0.17	10.9±0.4	−20.7±0.2‰	−24.3±0.5‰

understand and constrain C export and cycling in these systems. It should be stressed that the above-mentioned estimates refer to the amounts of carbon transported to the estuarine zone (which holds true for all other riverine C flux estimates for African rivers), but do not take into account the local processing (removal and/or addition) of carbon in the estuarine mixing zone. As we will argue further on, such processes are clearly evident from our data set, both for the Tana estuary and for the delta region.

Carbon sources in the Tana estuary and delta—The carbon stable isotope composition of particulate organic matter in estuaries is frequently used as a tracer of the origin of C, and may distinguish terrestrial sources (∼−28‰ for C3 vegetation) from marine inputs (with typical values ranging between −21 and −18‰). As a result of methodological constraints, $\delta^{13}C$ data on DOC from rivers and estuaries are still very scarce (e.g., Raymond and Bauer 2001; Otero et al. 2003), but several recent studies have indicated that substantial differences may exist in the sources of POC and DOC in rivers and estuaries (e.g., Bianchi et al. 2004; Ziegler and Brisco 2004; Mayorga et al. 2005). In our case, the $\delta^{13}C$ of the POC pool in the freshwater part of the Tana is much more enriched in ^{13}C than would be expected from C3-dominated terrestrial vegetation, indicating that C4 inputs from upland and/or surrounding grasslands contribute substantially to the transported organic carbon load. By using an end-member value of −12.8‰ for C4-derived carbon (based on regional data from Tieszen et al. 1979 and Muzuka 1999) and a typical value of −28.2‰ for C3 vegetation (e.g., Bouillon et al. 2004 for mangroves), we estimate that C4-derived matter contributes 50 ± 11% to the POC pool in the delta creeks (range: 26–72%), 40 ± 6% in the freshwater part and inner estuary of the Tana (range: 29–47%), and 49 ± 4% in the Tana plume (range: 43–57%). Similarly, intertidal sediments under the mangrove vegetation in the area were found to contain significant amounts of C4-derived carbon (36–46% in the delta, ∼15% along the Tana proper; Table 2). In these calculations, we do not consider a significant contribution by phytoplankton biomass as a potential explanation for the high $\delta^{13}C_{POC}$ values–for the Tana and Matolo, the high turbidity and POC : Chl *a* ratios (Fig. 5A, 8B) indicate that a substantial contribution of phytoplankton can be easily excluded. For the tidal creeks in the delta, the higher Chl *a* concentrations and lower POC : Chl *a* ratios (Fig. 8A, B) do not allow us to exclude a certain contribution by phytoplankton to the POC pool, but considering the low $\delta^{13}C_{DIC}$ values in these creeks (mostly between −4 and −11‰; Fig. 3E), this should result in a distinctly negative $\delta^{13}C$ signature for local phytoplankton biomass (roughly −24 to −31‰), and we therefore assume that the bias in our estimates of the C4 contribution to the POC and DOC pool in these creeks, because phytoplankton biomass is not considered, should be limited.

For the DOC pool, however, the $\delta^{13}C$ data indicate a surprising difference in its origin compared with the POC data. In most cases, the $\delta^{13}C_{DOC}$ values are consistently more negative than the $\delta^{13}C_{POC}$ signatures (Fig. 7A, B, C), suggesting a substantially lower contribution by C4-derived carbon, which was estimated at 27 ± 7% (range: 18–46) for the freshwater part and inner Tana estuary, 13 ± 7% (range: 1–25) for the Tana plume, and 29 ± 12% (range: 10–56%) for the Tana Delta surface waters. The pore water $\delta^{13}C_{DOC}$ data from both the Tana estuary mangroves and those in the southern delta are all close to or within the expected range for C3-derived material and thus indicate only a minor contribution by C4-derived carbon (at most 5–16% according to the above mixing calculations), whereas the sediment TOC data indicated a substantial contribution of C4 material in the delta mangrove sediments (36–46%, *see above* and Table 2).

When looking at the profiles of $\delta^{13}C_{POC}$ and $\delta^{13}C_{DOC}$ along the salinity gradient of Matolo Creek and the Tana (Fig. 7A, B), two different patterns emerge: first, for the Tana estuary, $\delta^{13}C_{POC}$ values show a gradual but slight increase along the salinity gradient, whereas $\delta^{13}C_{DOC}$ values show a consistent and larger decrease (Fig. 7A), thus leading to an increasing difference in their sources along the salinity gradient; and second, for Matolo Creek, $\delta^{13}C_{POC}$ values show no gradient, whereas $\delta^{13}C_{DOC}$ is consistently more negative than $\delta^{13}C_{POC}$ and shows a clear nonconservative decrease in the 15–30 salinity zone (Fig. 7B), coinciding with a net addition of DOC (Fig. 5E).

Differences in the contribution of C4 material to the POC and DOC pools have also been proposed recently for the Mississippi River, where high-molecular-weight DOC was found to contain a significantly lower contribution by C4 material than the POC pool (Bianchi et al. 2004), although the data of Kendall et al. (2001) suggest that the Mississippi POC pool contains less C4-derived material than indicated by the data of Bianchi et al. (2004). Although the latter authors suggested that C4 material could be more strongly bound to fine suspended matter and that this might offer a physical protection against microbial

decay (inhibiting its conversion to DOC), we propose that other mechanisms may be responsible for such differences. The patterns observed would also be consistent with significant inputs of C4 material via freshwater inputs, whereby the composition of the particulate pool remains more stable as a result of its association with the mineral phase, but where the DOC composition is more strongly impacted by local inputs by, e.g., mangrove-derived DOC, and/or whereby C4-derived DOC is selectively mineralized because C4 material has been reported to be more labile than C3 material (*see* Mayorga et al. 2005 and references therein). Such a scenario would be consistent with the observed patterns of $\delta^{13}C_{POC}$ and $\delta^{13}C_{DOC}$ along the Tana and Matolo Creek (Fig. 7A, B).

Although a major contribution of C4-derived carbon was not unexpected for the Tana River (given that large parts of the drainage basin consist of savanna grasslands), the C4 contribution to the POC and (albeit to a lesser extent) DOC pool in the delta contrasts with our expectation that increased inputs of organic matter would mainly result from local mangrove production. Whether the high C4 inputs observed are of local nature (i.e., grasslands from within the delta) or originate from upstream cannot be unambiguously deduced from our data, but the nonconservative nature of the POC and DOC profiles (Fig. 5B, 5E) suggest that they are at least in part local. In any case, the fact that C4 inputs contribute strongly to the POC and DOC load is important for the interpretation of marine sedimentary records along the east African coast because the stable isotope signature of the transported terrestrial material is likely indistinguishable from marine phytoplankton production. Recognition of C4-derived terrestrial inputs in the Gulf of Mexico has recently indicated that terrestrial inputs in this area had been previously underestimated (Goñi et al. 1998). Finally, the marked differences in the origin of DOC and POC stresses the need for isotopic characterization of both pools in future studies of estuarine carbon cycling, which will likely become feasible considering the recent introduction of automated setups for $\delta^{13}C_{DOC}$ analysis (St-Jean 2003; Bouillon et al. 2006).

The increase of silica in oligo- and mesohaline regions is a common feature in both temperate (e.g., Anderson 1986; Meybeck et al. 1988; Clark et al. 1992) and tropical estuaries (e.g., Eyre and Balls 1999; Dittmar and Lara 2001). This input of silica is usually attributed to pelagic and/or benthic remineralization of freshwater diatoms that die in the oligohaline region of the estuary either to haline stress and/or light limitation in the maximum turbidity zone. The observed increase of silica in the Tana (Fig. 9A) seems to be due the remineralization of organic matter as it coincides with an increase of phosphate (Fig. 9B) and a decrease of both Chl *a* (Fig. 8A) and POC (Fig. 5B). The observed decrease of Chl *a* (about 1.5 μg Chl *a* L^{-1}) would correspond to an increase in silica of only 4 μmol L^{-1}, assuming a POC : Chl *a* ratio of 40 (Abril et al. 2002) and Si : C molar ratio of 0.79 for freshwater diatoms (Sicko-Goad et al. 1984). The observed decrease of POC (about 13 mg L^{-1}), on the other hand, would correspond to an increase in silica ranging between 13 and 43 μmol L^{-1}, assuming a Si : C molar ratio ranging between 0.012 and 0.040 for terrestrial plant organic matter (Conley 2002). Although the increase of silica could be due to benthic remineralization of freshwater diatoms, these computations strongly suggest that there is a significant contribution of degradation of terrestrial plant organic matter to the observed increase in silica of about 100 μmol L^{-1}. Similarly, the increase of phosphate in the Tana oligohaline region of about 1 μmol L^{-1} is more consistent with the degradation of terrestrial plant organic matter rather than freshwater phytoplankton. This increase of phosphate could also be due to desorption from suspended particles, although this process occurs in the mesohaline region (e.g., Froelich 1988), and on the contrary abiotic removal can occur in the oligohaline region (e.g., Fox et al. 1986). The decrease of POC would correspond to an increase of phosphate of about 1.3 μmol L^{-1} assuming a P : C molar ratio of 1 : 852 for terrestrial plant organic matter (Cross et al. 2003). The decrease of Chl *a* would lead an increase of phosphate of only 0.05 μmol L^{-1}, assuming a P : C molar ratio of 1 : 100 for freshwater phytoplankton (Lampman et al. 2001). The input of silica to the ocean in the form of phytoliths from terrestrial plants has been assumed to be significant in the global marine silica cycle (Alexandre et al. 1997; Conley 2002). Our results thus suggest that a significant conversion of terrestrial plant biogenic silica to dissolved silica could occur in estuaries.

Mineralization and CO_2 efflux: magnitude and sources—pCO_2 values indicate a strong oversaturation in the freshwater part of the Tana River (4,390 ± 660 ppm), and decreased rapidly toward the river plume where values close to equilibrium were reached (Fig. 3D). Compared with the Tana, pCO_2 values in Matolo Creek and the mangrove creeks of the delta were much higher at similar salinities, with an overall average of 2,600 ± 1,750 ppm. pCO_2 data were used to estimate the flux of CO_2 (F) across the water-air boundary according to: $F = k \alpha \Delta pCO_2$ where k is the gas transfer velocity, α the solubility coefficient for CO_2, and ΔpCO_2 represents the difference in partial pressure of CO_2 between water and air. k values in coastal environments are known to be to a large extent determined by wind speed and other site-specific factors such as water currents and fetch-limitation (*see* Borges et al. 2004 for a recent discussion). Because no concurrent wind speed measurements were taken, we used a constant k value of 4 cm h^{-1}. We must stress that this value is in the lower range of k values reported for estuaries and tidal creeks (Borges et al. 2003), and will therefore result in conservative (i.e., minimal) CO_2 flux estimates. Our calculations result in an estimated water-air CO_2 flux of 116 ± 12 mmol m^{-2} d^{-1} in the freshwater part of the Tana estuary (rapidly decreasing toward the plume to 4.1 ± 6.4 mmol m^{-2} d^{-1} at salinities >20). In the delta, the overall average CO_2 flux was estimated at 58 ± 45 mmol m^{-2} d^{-1} (with extremes of 3 and 252 mmol m^{-2} d^{-1}), which is in line with the global estimate of ~50 mmol m^{-2} d^{-1} proposed by Borges et al. (2003) for open waters surrounding mangroves.

Although the limited number of respiration/production data (Table 1) are not depth-integrated and are too few to

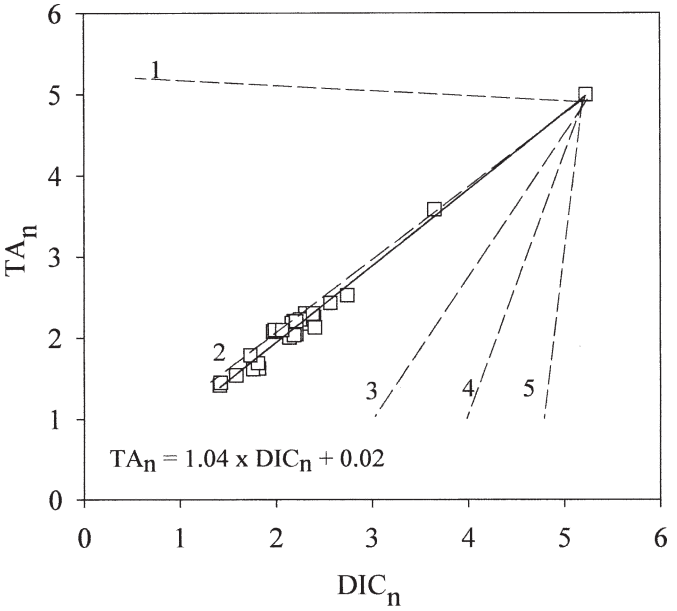

Fig. 10. Salinity-normalized TA and DIC for surface waters in southern delta creeks. Solid line represents linear regression on these data; dotted lines correspond to theoretical covariation of TA_n and DIC_n for various potentially acting processes: (1) aerobic respiration, (2) sulfate reduction, (3) $CaCO_3$ dissolution, (4) Mn reduction, and (5) Fe reduction.

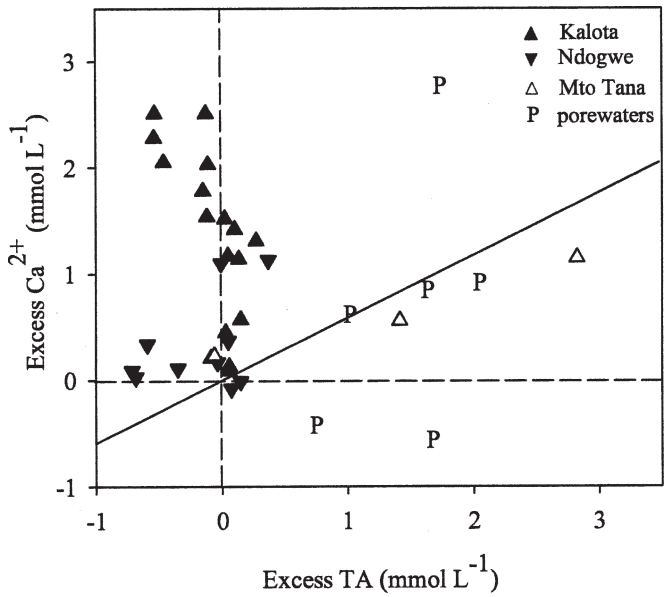

Fig. 11. Relationship between excess total alkalinity and excess Ca^{2+} for surface waters in southern delta creeks. Excess TA and Ca^{2+} were calculated on the basis of difference between actual measurements and those predicted based on salinity and conservative mixing. Solid line represents stoichiometry predicted by carbonate dissolution.

conclusively state that the aquatic metabolism is insufficient to explain the observed CO_2 efflux, the range of values and the absence of a relationship between R and pCO_2 or $\%O_2$ do not support the idea that the high pCO_2 and other heterotrophic signatures of the creek waters are only determined by the metabolism of the water column. The same is indicated by some of the $\delta^{18}O_{DO}$ values, which suggest a significant role for photosynthesis in some of the tidal creeks. Instead, our observations would be consistent with the scenario proposed by Cai et al. (1999) for estuarine marshes, whereby the high pCO_2 and low $\%O_2$ imposed by the large intertidal areas during inundation are reflected in the tidal creek water column. Further evidence for this scenario is provided by the covariation between salinity normalized TA (TA_n) and DIC (DIC_n) (Fig. 10), which follows a stoichiometry dependent on the biogeochemical processes underlying their variation (Borges et al. 2003). The TA_n and DIC_n values for the tidal creeks in the delta are well correlated (Fig. 10) and are close to the pattern expected when sulfate reduction would be the dominant process acting on their dynamics. Although these data can similarly be explained by a combination of aerobic mineralization and other diagenetic processes, it is clear that such anaerobic diagenetic processes occurring in the intertidal sediments must be invoked to explain the TA and DIC variations, and similar patterns have been found in other tidal mangrove creeks (Borges et al. 2003; A. V. Borges and S. Bouillon unpubl. data from mangrove systems in Kenya, Tanzania, and Vietnam). The pore-water data from the intertidal mangrove areas are also in line with such a scenario: all pore waters showed anoxic or near-anoxic conditions, with low pH, high TA, DIC, and pCO_2. These are indicative of high metabolic activity in the sediments, and during inundation this should result in a depletion of water column O_2 and a net flux of DIC and CO_2 from the sediment to the water column, which will subsequently be reflected in the creek water column when the water retreats. Therefore, as Neubauer and Anderson (2003) point out, oversaturation of CO_2 and undersaturation of O_2 in tidal creek waters are not necessarily due to net heterotrophy of the water column.

The dissolution of $CaCO_3$ has been assumed to be a significant process in the sediments of the mangrove forests in Gazi Bay on the basis of pore-water pH and sediment $CaCO_3$ content (Middelburg et al. 1996). In other mangrove environments, creek water DIC and TA covariation suggests a significant impact of diagenetic processes, although stoichiometrically inconsistent with $CaCO_3$ dissolution, as discussed above. Both Ca^{2+} and Mg^{2+} showed conservative behavior along the salinity gradient of the Tana and Matolo Creek. Several creeks and pore-water stations in the southern delta, however, showed marked nonconservative behavior of Ca^{2+} (whereas Mg^{2+} was conservative throughout). In the majority of surface and pore-water samples from the delta, Ca^{2+} was in excess, and the difference in the actual Ca^{2+} concentration and that calculated on the basis of conservative mixing reached $+1.41 \pm 0.79$ mmol L^{-1} for Kalota Creek and $+0.92 \pm 1.19$ mmol L^{-1} for the mangrove pore waters. Carbonate dissolution ($CaCO_3 + CO_2 + H_2O <=> 2\ HCO_3^- + Ca^{2+}$) generates TA in a stoichiometry of 2 mmol TA per mmol of $CaCO_3$ dissolved. Because the TA profile does not follow the same trend as for Ca^{2+} (Fig. 3C, F), and given the lack of correlation between excess TA and excess Ca^{2+} (Fig. 11), this suggests that the excess Ca^{2+} is in the majority of

samples not the result of $CaCO_3$ dissolution. An alternative explanation is that dissolution of evaporites such as gypsum ($CaSO_4$), characteristic of evaporative environments such as the salt pans found in parts of the delta in particular around Kalota Creek, is responsible for the nonconservative Ca^{2+} profiles.

The pattern in $\%O_2$ is largely in agreement with the stable oxygen isotope data (Fig. 4). $\delta^{18}O_{DO}$ is influenced both by air-water exchange (under equilibrium conditions, the theoretical $\delta^{18}O_{DO}$ value would be +24.2‰), photosynthesis (which produces O_2 with a $\delta^{18}O$ signature similar to that of the source water, thereby typically lowering the $\delta^{18}O_{DO}$; Guy et al. 1993), and oxygen consumption by respiration, which fractionates by ~18‰ and thereby leaves the residual O_2 pool enriched in ^{18}O (e.g., Quay et al. 1995; Wang and Veizer 2000). Under the (simplifying) assumption that both $\delta^{18}O_{DO}$ and $\%O_2$ are constant over time, the combination of both parameters has been used in freshwater systems to estimate the metabolic balance of the water column (Quay et al. 1995; Wang and Veizer 2000), Application of this approach to our data from the Tana freshwater samples (salinity < 1.8) results in an estimated P : R ratio of 0.42 ± 0.08 ($n = 9$; one outlier removed), although it must be stressed here that the underlying assumption of steady-state conditions is unlikely to be valid for such a dynamic and biogeochemically active system, and application of this approach would ideally be based on diurnal patterns of $\%O_2$ and $\delta^{18}O$ (Parker et al. 2005). In estuaries, however, the application of $\delta^{18}O_{DO}$ data for quantitative estimates of the aquatic metabolism is substantially more complicated. However, as a simple rule of thumb, we can state that $\delta^{18}O_{DO}$ values above +24.2‰ indicate the predominance of respiration over photosynthesis, whereas values lower than +24.2‰ show the effect of photosynthetic O_2. The latter does not necessarily imply that photosynthesis exceeds respiration, however, as the effect of the removal of a given amount of O_2 by respiration (which fractionates by 18 ± 3‰, *see above*) can be somewhat less pronounced that the addition of a similar amount of photosynthetically produced O_2, the latter having the same $\delta^{18}O$ signature as the source water, i.e., in our case ranging between −2.1‰ for the freshwater endmember to +0.4‰ for the most marine samples (data not shown). Nevertheless, ~25% of the $\delta^{18}O_{DO}$ data from the delta (and several samples from the Tana plume) show values lower than +24.2‰, indicating that photosynthetically produced O_2 contributes to the dissolved oxygen pool and that the metabolic balance is likely close to 1. This is in line with the idea that the high pCO_2 values in the water column are partially sustained by mineralization in the intertidal areas. Note that measured R values are at the lower end of the range of values reported in tropical estuaries, 9–75 μmol O_2 L^{-1} d^{-1} in the Celestun Lagoon and 23–150 μmol O_2 L^{-1} d^{-1} in the Fly River Delta (Hopkinson and Smith 2005).

The pCO_2 values in the freshwater end of the Tana River ($4{,}390 \pm 660$ ppm) are in the higher end of the range reported for rivers worldwide (e.g., *see* compilations in Cole and Caraco 2001; Abril and Borges 2004), and are likely to be sustained by the high organic carbon load, which appears to be mainly composed of degraded terrestrial (C3- and C4-derived) material. The high pCO_2 in the tidal creeks of the delta is consistent with similar data from other mangrove systems (Borges et al. 2003; Bouillon et al. 2003); however, in previous studies we assumed that the enhanced CO_2 efflux in mangrove creeks was likely to be directly linked to higher organic carbon inputs from local mangrove production. The high contribution of C4 material in the suspended, dissolved and sedimentary organic carbon pool in this system raises the question whether this C4 material also contributes to local mineralization and the subsequent high CO_2 efflux in the tidal creeks. Considering the above-mentioned scenario where mineralization in the intertidal areas is likely a significant component of the observed water column chemistry, we compared DIC and $\delta^{13}C_{DIC}$ data of pore waters in the delta with those in surface waters of similar salinity to estimate the $\delta^{13}C$ value of the excess DIC, thereby assuming that the excess DIC can be attributed solely to mineralization. These calculations result in an average $\delta^{13}C$ signature for the respired C source of −23.5‰, i.e., with an estimated contribution of 30% by C4-derived carbon, within the range of values calculated for the contribution of C4 material to the sediment TOC and water column POC and DOC pools (*see above*). The latter estimates are also consistent with $\delta^{13}C$ data on bacterial biomarkers (data presented in Bouillon and Boschker 2006), which indicated similar $\delta^{13}C$ values for the bacterial C substrate in these intertidal sediments. On the other hand, it should be noted that DOC concentrations in these pore waters are typically high (Fig. 5E) and were shown to be predominantly derived from local mangrove vegetation (Fig. 5F, *see above*). This pattern raises the question to what extent local sources of particulate and dissolved organic carbon contribute to fueling bacterial mineralization in these intertidal sediments (*see also* Bouillon and Boschker 2006). Although our data suggest a larger role for the particulate pool, a more comprehensive data set on the stable isotope composition of both sediment TOC, pore-water DOC, and epiphytic algal and bacterial markers from a range of sedimentary environments would be needed. Thus, mineralization and subsequent CO_2 efflux in these tidal creeks appear to be partially sustained by local mangrove inputs, but with a substantial contribution by C4-derived organic matter, either from the surrounding savanna grasslands or transported from further upstream. In other systems where the catchment is dominated by C3 vegetation, this would not have been evident in the $\delta^{13}C$ data, but our data indicate that the high pCO_2 typically observed in mangrove systems is not necessarily linked entirely to the high local inputs of mangrove production, but might also be linked to the higher residence time, which could favor degradation of organic material transported via freshwater inputs.

The Tana River carried a high suspended matter and particulate organic carbon load, the latter being composed of roughly equal contributions by C3- and C4-derived material. Similarly, organic carbon in the tidal mangrove creeks of the delta contained a surprisingly large fraction of

C4-derived vascular plant material. In contrast, the DOC pool in both systems was found to be consistently more depleted in ^{13}C, indicating a lower contribution of C4-derived material, and pore-water DOC in mangrove sediments was found to be predominantly mangrove derived, even in sites where C4 material made a substantial contribution to the sediment TOC pool. Because our data were collected during a single sampling campaign, seasonal variations in the relative contribution of C3 and C4 material cannot be considered. Our tentative estimates for organic and inorganic carbon export rates from the Tana were far higher than those currently in use for the tropical east African zone, and DIC : POC ratios were almost 15 times higher than those proposed by Ludwig et al. (1996*a,b*), which were based on an empirical model. Given the absence of actual data on other riverine systems in the region, it appears evident that more data are needed to better constrain suspended matter, and carbon and nutrient fluxes to the Indian Ocean from this region. During estuarine mixing, significant changes in the sources of DOC and POC were found, stressing that intense processing taking place in estuaries and tidal creeks may cause large differences between the riverine organic matter and that are ultimately exported to the coastal zone. Our data further indicate a strong heterotrophic signature in the water column, in particular for the freshwater part of the Tana River and the tidal mangrove creeks in the southern delta, resulting in a high CO_2 efflux. However, part of this signature is suggested to be related to the strong interaction with the large intertidal areas, as proposed for estuarine salt marshes by Cai et al. (1999) and for freshwater marshes by Neubauer and Anderson (2003). Mineralization in both the Tana River and the delta appears to be sustained by both C3/mangrove inputs and a significant contribution by C4-derived organic matter.

References

Abril, G., and A. V. Borges. 2004. Carbon dioxide and methane emissions from estuaries, p. 287–207. *In* Tremblay. A, L. Varfalvy, C. Roehm, and M. Garneau [eds.], Greenhouse gases emissions from natural environments and hydroelectric reservoirs: Fluxes and processes. Environmental Science Series. Springer.

———, E. Nogueira, H. Hetcheber, G. Cabeçadas, E. Lemaire, and M. J. Brogueira. 2002. Behaviour of organic carbon in nine contrasting European estuaries. Estuar. Coast. Shelf Sci. **54:** 241–262.

Alexandre, A., J.-D. Meunier, F. Colin, and J.-M. Koud. 1997. Plant impact on the biogeochemical cycle of silicon and related weathering processes. Geochim. Cosmochim. Acta **61:** 677–682.

Anderson, G. F. 1986. Silica, diatoms and a freshwater productivity maximum in Atlantic coastal plain estuaries, Chesapeake Bay. Estuar. Coast. Shelf Sci. **22:** 183–197.

Bianchi, T. S., T. Filley, K. Dria, and P. G. Hatcher. 2004. Temporal variability in sources of dissolved organic carbon in the lower Mississippi River. Geochim. Cosmochim. Acta **68:** 959–967.

Borges, A. V. 2005. Do we have enough pieces of the jigsaw to integrate CO_2 fluxes in the Coastal Ocean? Estuaries **28:** 3–27.

———, B. Delille, L. S. Schiettecatte, F. Gazeau, G. Abril, and M. Frankignoulle. 2004. Gas transfer velocities of CO_2 in three European estuaries (Randers Fjord, Scheldt and Thames). Limnol. Oceanogr. **49:** 1630–1641.

———, S. Djenidi, G. Lacroix, J. Théate, B. Delille, and M. Frankignoulle. 2003. Atmospheric CO_2 flux from mangrove surrounding waters. Geophys. Res. Lett. **30:** 1558.

Bouillon, S., and H. T. S. Boschker. 2006. Bacterial carbon sources in coastal sediments: A meta-analysis based on stable isotope data of biomarkers. Biogeosciences **3:** 175–185.

———, M. Frankignoulle, F. Dehairs, B. Velimirov, A. Eiler, H. Etcheber, G. Abril, and A. V. Borges. 2003. Inorganic and organic carbon biogeochemistry in the Gautami Godavari estuary (Andhra Pradesh, India) during pre-monsoon: The local impact of extensive mangrove forests. Glob. Biogeochem. Cycles **17:** 1114.

———, T. Moens, I. Overmeer, N. Koedam, and F. Dehairs. 2004. Resource utilization patterns of epifauna from mangrove forests with contrasting inputs of local versus imported organic matter. Mar. Ecol. Prog. Ser. **278:** 77–88.

———, M. Korntheuer, and F. Dehairs. 2006. A new automated setup for stable isotope analysis of dissolved organic carbon. Limnol. Oceanogr. Methods **4:** 216–226.

Cai, W. J., L. R. Pomeroy, M. A. Moran, and Y. Wang. 1999. Oxygen and carbon dioxide mass balance for the estuarine–intertidal marsh complex of five rivers in the southeastern U.S. Limnol. Oceanogr. **44:** 639–649.

Clark, J. F., H. J. Simpson, R. F. Bopp, and B. Deck. 1992. Geochemistry and loading history of phosphate and silicate in the Hudson Estuary. Estuar. Coast. Shelf Sci. **34:** 213–233.

Conley, D. J. 2002. Terrestrial ecosystems and the global biogeochemical silica cycle. Glob. Biogeochem. Cycles **16:** 1121.

Cole, J. J., and N. F. Caraco. 2001. Carbon in catchments: Connecting terrestrial carbon losses with aquatic metabolism. Mar. Freshwat. Res. **52:** 101–110.

Colombini, I., R. Berti, A. Ercolini, A. Nocita, and L. Chelazzi. 1995. Environmental factors influencing the zonation and activity patterns of a population of *Periophthalmus sobrinus* Eggert in a Kenyan mangrove. J. Exp. Mar. Biol. Ecol. **190:** 135–149.

Cross, W. F., J. P. Benstead, A. D. Rosemond, and J. B. Wallace. 2003. Consumer-resource stoichiometry in detritus-based streams. Ecol. Lett. **6:** 721–732.

Denhardt, C., and G. Denhardt. 1884. Bemerkungen zur Originalkarte des unteren Tana-Gebietes. Zeitsch. Gesellschaft Erdkunde (Berl.) **19:** 122–160.

Dittmar, T., and R. J. Lara. 2001. Do mangroves rather than rivers provide nutrients to coastal environments south of the Amazon River? Evidence from long-term flux measurements. Mar. Ecol. Prog. Ser. **213:** 67–77.

Eyre, B., and P. Balls. 1999. A comparative study of nutrient behavior along the salinity gradient of tropical and temperate estuaries. Estuaries **22:** 313–326.

Fox, L. E., S. L. Sager, and S. C. Wofsy. 1986. The chemical control of soluble phosphorus in the Amazon estuary. Geochim. Cosmochim. Acta **50:** 783–794.

Frankignoulle, M., and A. V. Borges. 2001. Direct and indirect pCO_2 measurements in a wide range of pCO_2 and salinity values (the Scheldt estuary). Aquat. Geochem. **7:** 267–273.

———, G. Abril, A. Borges, I. Bourge, C. Canon, B. Delille, E. Libert, and J.-M. Théate. 1998. Carbon dioxide emission from European estuaries. Science **282:** 434–436.

Froelich, P. N. 1988. Kinetic control of dissolved phosphate in natural rivers and estuaries: A primer on the phosphate buffer mechanism. Limnol. Oceanogr. **33:** 649–668.

Goñi, M. A., K. C. Ruttenberg, and T. I. Eglinton. 1998. A reassessment of the sources and importance of land-derived organic matter in surface sediments from the Gulf of Mexico. Geochim. Cosmochim. Acta **62:** 3055–3075.

Grasshoff, K., M. Ehrhardt, and K. Kremling. 1983. Methods of seawater analysis. Verlag Chemie.

Guy, R. D., M. L. Fogel, and J. A. Berry. 1993. Photosynthetic fractionation of the stable isotopes of oxygen and carbon. Plant Physiol. 101, 37–47.

Hopkinson, C. S. J., and E. M. Smith. 2005. Estuarine respiration: An overview of benthic, pelagic and whole system respiration, p. 123–157. *In* P. A. del Giorgio and P. J. L. Williams [eds.], Respiration in aquatic ecosystems. Oxford Univ. Press.

Ittekkot, V., and R. W. P. M. Laane. 1991. Fate of riverine particulate organic matter, p. 233–243. *In* E. T. Degens, S. Kempe and J. E. Richey [eds.], Biogeochemistry of major world rivers. Wiley.

Jennerjahn, T. C., and V. Ittekkot. 2002. Relevance of mangroves for the production and deposition of organic matter along tropical continental margins. Naturwissenschaften **89:** 23–30.

Kendall, C., S. R. Silva, and V. J. Kelly. 2001. Carbon and nitrogen isotopic compositions of particulate organic matter in four large river systems across the United States. Hydrol. Proc. **15:** 1301–1346.

Kitheka, J. U., M. Obiero, and P. Nthenge. 2005. River discharge, sediment transport and exchange in the Tana estuary, Kenya. Estuar. Coast. Shelf Sci. **63:** 455–468.

Lampman, G. G., N. F. Caraco, and J. J. Cole. 2001. A method for the measurement of particulate C and P on the same filtered sample. Mar. Ecol. Prog. Ser. **217:** 59–65.

Ludwig, W., P. Amiotte-Suchet, and J. L. Probst. 1996*b*. River discharges of carbon to the world's oceans: Determining local inputs of alkalinity and of dissolved and particulate organic carbon. C. R. Acad. Sci. Paris II **323:** 1007–1014.

———, J. L. Probst, and S. Kempe. 1996*a*. Predicting the oceanic input of organic carbon by continental erosion. Glob. Biogeochem. Cycles **10:** 23–41.

Maingi, J. K., and S. E. Marsh. 2002. Quantifying hydrologic impacts following dam construction along the Tana River, Kenya. J. Arid Environ. **50:** 53–79.

Martins, O., and J. L. Probst. 1992. Biogeochemistry of major African rivers: Carbon and mineral transport, p. 127–155. *In* Degens E. T., S. Kempe, and J. E. Richey [eds.], Biogeochemistry of major world rivers. Wiley.

Mayorga, E., A. K. Aufdenkampe, C. A. Masiello, A. V. Krusche, J. I. Hedges, P. D. Quay, J. E. Richey, and T. A. Brown. 2005. Young organic matter as a source of carbon dioxide outgassing from Amazonian rivers. Nature **436:** 538–541.

Meybeck, M., G. Cauwet, S. Dessery, M. Somville, D. Gouleau, and G. Billen. 1988. Nutrients (organic C, P, N, Si) in the eutrophic River Loire (France) and its estuary. Estuar. Coast. Shelf Sci. **27:** 595–624.

Middelburg, J. J., J. Nieuwenhuize, F. J. Slim, and B. Ohawa. 1996. Sediment biogeochemistry in an East African mangrove forest (Gazi Bay, Kenya). Biogeochemistry **34:** 133–155.

Miyajima, T., Y. Yamada, Y. T. Hanba, K. Yoshii, T. Koitabashi, and E. Wada. 1995. Determining the stable-isotope ratio of total dissolved inorganic carbon in lake water by GC/C/IRMS. Limnol. Oceanogr. **40:** 994–1000.

Muzuka, A. N. N. 1999. Isotopic composition of tropical east African flora and their potential as source indicators of organic matter in coastal marine sediments. J. Afr. Earth Sci. **28:** 757–766.

Neubauer, S. C., and I. C. Anderson. 2003. Transport of dissolved inorganic carbon from a tidal freshwater marsh to the York River estuary. Limnol. Oceanogr. **48:** 299–307.

Otero, E., R. Culp, J. Noakes, and R. E. Hodson. 2003. The distribution and $\delta^{13}C$ of dissolved organic carbon and its humic fraction in estuaries of southeastern USA. Estuar. Coast. Shelf Sci. **56:** 1187–1194.

Ovalle, A. R. C., C. E. Rezende, L. D. Lacerdea, and C. A. R. Silva. 1990. Factors affecting the hydrochemistry of a mangrove tidal creek, Sepetiba Bay, Brazil. Estuar. Coast. Shelf Sci. **31:** 639–650.

Parker, S. R., S. R. Poulton, C. H. Gammons, and M. D. Degrandpre. 2005. Biogeochemical controls on diel cycling of stable isotopes of dissolved O_2 and dissolved inorganic carbon in the Big Hole River, Montana. Environ. Sci. Technol. **39:** 7134–7140.

Quay, P. D., D. O. Wilbur, J. E. Richey, A. H. Devol, R. Benner, and B. R. Forsberg. 1995. The $^{18}O:^{16}O$ of dissolved oxygen in rivers and lakes in the Amazon Basin: Determining the ratio of respiration to photosynthesis in freshwaters. Limnol. Oceanogr. **40:** 718–729.

Raymond, P. A., and J. E. Bauer. 2001. Use of ^{14}C and ^{13}C natural abundances for evaluating riverine, estuarine, and coastal DOC and POC sources and cycling: A review and synthesis. Org. Geochem. **32:** 469–485.

Richey, J. E., J. M. Melack, A. K. Aufdenkampe, M. V. Ballester, and L. L. Hess. 2002. Outgassing from Amazonian rivers and wetlands as a large tropical source of atmospheric CO_2. Nature **416:** 617–620.

Sampson, H. C. 1933. The Tana River region of Kenya Colony. J. R. Soc. Arts **84:** 92–111.

Schlünz, B., and R. R. Schneider. 2000. Transport of terrestrial organic carbon to the oceans by rivers: Re-estimating flux- and burial rates. Int. J. Earth Sci. **88:** 599–606.

Sicko-Goad, L. M., C. L. Schelske, and E. F. Stoermer. 1984. Estimation of intracellular carbon and silica content of diatoms from natural assemblages using morphometric techniques. Limnol. Oceanogr. **29:** 1170–1178.

St-Jean, G. 2003. Automated quantitative and isotopic (^{13}C) analysis of dissolved inorganic carbon and dissolved organic carbon in continuous-flow using a total organic carbon analyser. Rapid Comm. Mass Spectrom. **17:** 419–428.

Syvitski, J. P. M., C. J. Vörösmarty, A. J. Kettner, and P. Green. 2005. Impact of humans on the flux of terrestrial sediment to the global coastal ocean. Science **308:** 376–380.

Tieszen, L. L., M. M. Senyimba, S. K. Imbamba, and J. H. Throughton. 1979. The distribution of C3 and C4 grasses and carbon isotope discrimination along and altitudinal and moisture gradient in Kenya. Oecologia **37:** 337–350.

Wang, X., and J. Veizer. 2000. Respiration/photosynthesis balance of terrestrial aquatic ecosystems, Ottawa area, Canada. Geochim. Cosmochim. Acta **64:** 3775–3786.

Ziegler, S. E., and S. L. Brisco. 2004. Relationships between the isotopic composition of dissolved organic carbon and its bioavailability in contrasting Ozark streams. Hydrobiologia **513:** 153–169.

Received: 25 November 2005
Accepted: 21 June 2006
Amended: 30 July 2006